X-ray absorption near-edge studies of substitution for Cu in $YBa_2(Cu_{1-x}M_x)_3O_{7-\delta}$ (M = Fe, Co, Ni, and Zn)

C. Y. Yang,* A. R. Moodenbaugh, Y. L. Wang, Youwen Xu, S. M. Heald, D. O. Welch, and M. Suenaga
Materials Science Division, Brookhaven National Laboratory, Upton, New York 11973

D. A. Fischer
EXXON PRT, Brookhaven National Laboratory, Upton, New York 11973

J. E. Penner-Hahn
Department of Chemistry, University of Michigan, Ann Arbor, Michigan 48109
(Received 30 January 1990)

We report x-ray absorption near-edge measurements of $YBa_2(Cu_{1-x}M_x)_3O_{7-\delta}$ (M=Fe, Co, Ni, and Zn). Our study is primarily to determine several important material parameters, i.e., the location of dopants, the valence of dopants, structural changes, modifications of electronic densities of states, and the distribution of holes, which are thought to be key factors for understanding mechanisms causing the suppression of superconductivity via metal doping. Our results indicate that each metal substituent has a preference for a specific Cu site or combination of sites. We find that Fe and Co preferentially substitute for the Cu(1) atom at the linear-chain site; Ni resides in both Cu(1) and Cu(2) (the plane site); Zn occupies only the plane position Cu(2). In all cases, the metal-oxygen bond lengths (Fe-O, Co-O, Ni-O, and Zn-O) and valence states of dopant (mainly Fe^{3+}, Co^{3+}, Ni^{2+}, and Zn^{2+}) show little dependence on dopant concentration. Metal doping also has little effect on the valence of copper. However, each dopant affects to a different degree the oxygen $2p$ states. The changes of the oxygen $2p$ states for Fe-, Co-, and Ni-doped samples may be related to a reduction of some oxygen hole states. This reduction is attributed to a redistribution of charge carriers in the chain layer and possibly an inhibition of charge transfer from the chains to the planes. However, Zn substitutions show no observable change in its valence and oxygen hole states, indicating a different mechanism for suppression of superconductivity. Several possible explanations are offered that may elucidate the large suppression of T_c in the Zn-doped case.

I. INTRODUCTION

Substitutions of $3d$ transition metals[1-3] into the Cu sites of $YBa_2Cu_3O_{7-\delta}$ (abbreviated 1:2:3 in the following) lead to a depression of T_c. The mechanism of suppression of T_c, which depends strongly on the nature of the dopants, is still not well understood. Fe and Co substitutions induce an orthorhombic-to-tetragonal phase transition near $x=0.03$ (or 3 at. %), but an orthorhombic structure is retained for Ni and Zn substitutions. It appears that the variation of T_c is not influenced by average crystal symmetry. It has been suggested[4] that the presence of magnetic impurities in the lattice breaks the Cooper pairs, thereby depressing T_c. However, nonmagnetic Zn suppresses T_c more than magnetic Fe, Co, or Ni. Thus, there is no strong evidence to link the depression of T_c to magnetic interactions in the high-T_c materials.

One possible explanation for the variation of T_c for different dopants is based on the site occupancies of substitutional elements. There are two distinct Cu sites, the linear-chain site Cu(1) forming O-Cu-O units between two Ba layers and the plane site Cu(2) forming CuO_2 sheets between Ba and Y layers. A common structural unit in all Cu-based oxide superconductors is the two-dimensional network of CuO_2 sheets. It is generally believed that the Cu(2) plane site plays a key role in superconductivity. It is known that Fe and Co preferentially substitute into the Cu(1) chain site, and superconductivity is relatively weakly depressed by these substitutions. The cases of the other two dopants, i.e., Ni and Zn, however, are less easily understood. First the substitution sites are not well established. More importantly, the depression of T_c due to substitution by Zn is relatively great, while that of Ni is small.

Another constructive approach to the understanding of the effect of the metal doping in 1:2:3 is to find out how the distribution of the holes is affected by different dopants. Because charge carriers are holes, a reasonable assumption is that T_c is correlated with hole concentration in the CuO_2 sheets. Band theory calculations have reported[5] that the electrical conduction of 1:2:3 is determined by the Cu($3d$)-O($2p$) hybridized states, which are thought to be responsible for superconductivity. Several studies have suggested[6,7] that the holes are primarily located at the O sites. Because the density of states near the Fermi level is closely related to the Cu-O bonds, substitutions for Cu by $3d$ metals may reduce or increase

hole content. In fact, it has been shown[8–10] that hole concentration decreases with doping of Fe, Co, and Ni, but increases with Zn. As a result, changes of hole content by metal doping may strongly affect the O hole states. Therefore, detailed knowledge of the modification of local densities of states of O via metal doping may give an important clue for understanding the depression of superconductivity.

X-ray absorption near-edge spectroscopy (XANES) can provide electronic and structural information around each type of atom in the high-T_c materials. In this study, we describe XANES measurements designed to determine the influence of substituents on the location of dopants, the valence of dopants, structural changes, and modifications of electronic densities of states. The influence of $3d$ metal doping on the number of oxygen holes is also examined.

In the following, we first describe sample preparation, characterization, and experimental details of XAS measurements in Sec. II. Then we present the results for each x-ray absorption edge including Fe, Co, Ni, Zn, and O K edges and discuss the significance of these results in Sec. III. In particular, we consider several possible mechanisms responsible for suppressing T_c due to metal doping. A brief summary (Sec. IV) concludes this paper.

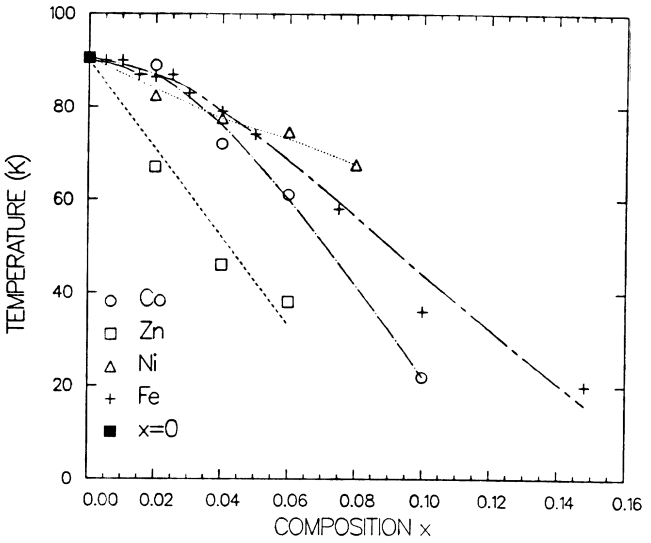

FIG. 1. Variation of T_c with substitution M (M = Fe, Co, Ni, and Zn) for Cu. Symbols for Fe are crosses, for Co are circles, for Ni are triangles, and for Zn are squares.

II. EXPERIMENT

A. Sample preparation and characterization

Dried Y_2O_3, CuO, and reagent $BaCO_3$ were combined along with Fe_2O_3, $CoCO_3$, $NiCO_3$, or ZnO in stoichiometric proportions. Then these powders were thoroughly ground and pelletized. The pellets were placed onto alumina boats and put into a box furnace set to 900 °C for about 20 h. The samples were reground, pelletized, and heat treated again at 900 °C. After a final regrinding and pelletizing, the samples were heated in flowing oxygen for 40 h near 970 °C, then for 8 h near 665 °C, with a furnace cool to below 100 °C.

A mutual inductance (ac susceptibility) apparatus was used to obtain superconducting transitions. The apparatus operates using an ac field near 200 Hz. Superconducting transition temperatures (T_c) are midpoints of the susceptibility transitions. The transition width (ΔT_c) is the temperature span between 10% and 90% of the susceptibility signal. As shown in Fig. 1, above 3% of metal substitutions effectiveness in reducing T_c is in the order T_c (Ni) < T_c (Fe) < T_c (Co) ≪ T_c (Zn). Clearly, Zn substitution has the most deleterious effect on T_c.

X-ray diffraction was performed using Cu K_α radiation on apparatus equipped with a diffracted beam monochromator. Lattice parameters were determined using a least-squares fit to peak positions. The variations of T_c, ΔT_c, and lattice parameters as a function of dopant concentration are listed in Table I. Above 3 at. % substitution with Fe and Co, a structural transition occurs from an orthorhombic to tetragonal structure, while with Ni- and Zn-doping samples maintain orthorhombic symmetry. This is consistent with the results of other authors.[1–3,9] Tetragonal parameters were refined when the orthorhombic splitting was not resolvable. Impurity peaks, which would have been visible if they had exceeded 1 at. % of the intensity of the most intense peak in the 1:2:3 pattern, were not observed in samples used in this study. Composition of the 1:2:3 phase was checked by electron microprobe equipped with a wavelength dispersive spectrometer. It was found that, in samples used in this work, the substituent (Fe, Co, Ni, or Zn) does enter the 1:2:3 phase. However, the total oxygen content was not determined for these samples.

B. X-ray absorption measurement

X-ray absorption measurements were performed on beam line X-19A of the National Synchrotron Light Source (NSLS) with a Si(220) double crystal monochromator. The details of the beam-line design have been published.[11] During this run, the NSLS was operated at an energy of 2.5 GeV and an electron current from 200 to 90 mA. The photon energy for each measurement was simultaneously calibrated from each corresponding metal foil, which was placed after the samples. The monochromator was detuned by reducing the incident photon flux about 20–30 % in order to suppress contamination from harmonics. The beam size was limited to $\sim 0.1 \times 10$ mm^2. We estimate the resolution of the monochromator to be 0.7 eV, 0.8 eV, 1.0 eV, and 1.2 eV at Fe, Co, Ni, and Zn edges, respectively. The data were measured in fluorescence mode with a nitrogen-filled ion chamber to monitor incident photon flux and a 13-element Ge detector[12] to monitor K_α x-rays from each edge. The advantage of using the energy dispersive Ge detector is it allows us to isolate unwanted fluorescence signals from the sample, such as Ba and Cu, thereby significantly improving the data quality. The XAS samples were ground to

TABLE I. Superconducting transition temperature T_c, and its width ΔT_c, and lattice parameters for metal-doped 1:2:3 samples.

M	x	T_c (K)	ΔT_c (K)	a (Å)	b (Å)	c (Å)
Cu	0	90.5	2	3.817	3.885	11.68
Fe	0.02	86.5	5	3.834	3.897	11.677
	0.03	83.0	6	3.852	3.861	11.686
	0.05	75.0	15	3.861		11.676
	0.10	36.0	20	3.867		11.686
	0.15	<4.2		3.873		11.660
Co	0.02	89.0	4	3.843	3.866	11.689
	0.04	73.0	16	3.863		11.677
	0.06	61.0	4	3.865		11.661
	0.10	26.0	22	3.873		11.682
	0.28	<4.2		3.888		11.636
Ni	0.02	82.5	2	3.818	3.886	11.676
	0.04	77.5	2	3.822	3.881	11.668
	0.06	74.5	2	3.821	3.880	11.666
	0.08	67.5	6	3.820	3.877	11.654
	0.10	60.0	6	3.823	3.888	11.659
Zn	0.01	78.0	5	3.817	3.885	11.681
	0.02	67.0	5	3.820	3.887	11.670
	0.04	46.0	15	3.823	3.887	11.677
	0.06	38.0	20	3.830	3.886	11.680
	0.10	12.0	12	3.826	3.888	11.690

fine powders ($\sim$400 mesh), and then spread uniformly onto Kapton tape. Samples were each measured over a period of 2–4 h. All spectra were taken at room temperature.

The vacuum oxygen K-edge XAS experiments were performed on the beam line U1 of the NSLS equipped with an extended-range grasshopper (ERG) monochromator. The ultrasoft XAS measurements were made using the fluorescence yield system shown in Fig. 2, which consists of a ballast region, window valve, soft x-ray proportional counter, and a sample chamber of small volume. The 0.1-μm-thick boron window, which is about 40% transmitting above the oxygen K edge, was used to isolate the ultrahigh vacuum synchrotron environment from the high-vacuum sample chamber. Although this system was originally designed for *in situ* high-pressure catalytic reaction studies, in this experiment it was utilized for rapid sample exchange, which is typically 2–5 min.[13] The proportional counter (PC) shown in Fig. 2 incorporates cylindrical electrode symmetry with a curved side window providing the ideal PC geometry for optimum energy resolution. The two cylindrical 1-μm-thick

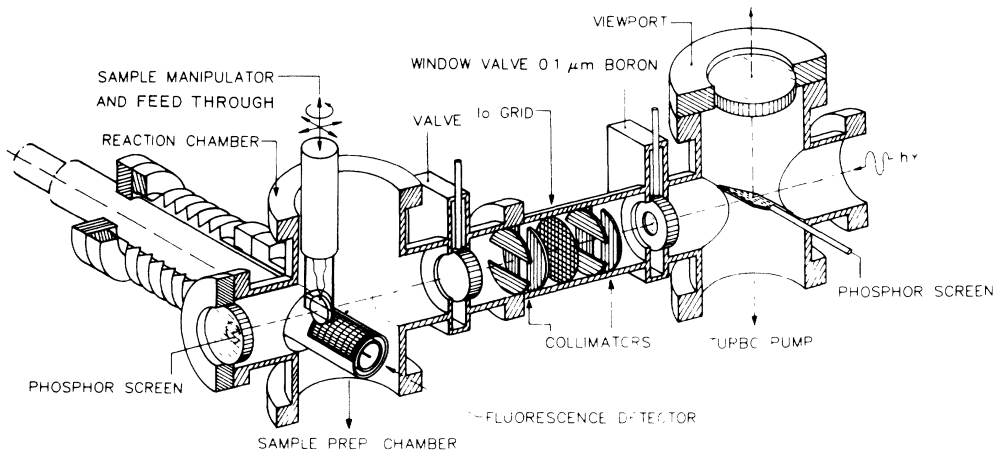

FIG. 2. Apparatus for ultrasoft fluorescence oxygen K-edge measurements.

polypropylene windows with a differentially pumped region between are supported by 90% transmitting electroformed stainless steel mesh and collected nearly 10% of the available solid angle. In addition, the side window geometry enables the PC to face the sample looking up, i.e., orthogonal to the plane of incidence away from the specular scattering peak. The energy dispersive characteristics of the proportional counter proved useful in separating the oxygen K_α fluorescence from the background copper L_α (excited in second order). After measurements, the T_c for each sample was remeasured. We find no evidence of a degradation of T_c for these samples, indicating that no significant oxygen was removed during data collection. This is due to the fact that the fluorescence technique used for these experiments is a bulk probe and is not sensitive to possible oxygen loss from the surface.

III. RESULTS AND DISCUSSION

A. Fe *K* edge

The details of XAS results for Fe substitution were reported earlier.[14] Three conclusions were drawn. First, the valence state of Fe is mainly +3 at all compositions. Second, Fe substitutes for the Cu(1) atom at the linear-chain site. There is no evidence for Fe residing at the Cu(2) plane site, even at higher Fe contents. Third, Fe-O-Fe linkage is observed. This is due to additional oxygen atoms being distributed in the chain layer. Similar conclusions were subsequently reported by Oyanagi *et al.*[15]

The XAS of Fe edge spectra of the 1*s*-3*d* transition for $YBa_2(Cu_{1-x}Fe_x)_3O_{7-\delta}$ support the above conclusions. It is well known[16] that the relative energies and intensities of 1*s*-3*d* edge features are determined by a number of considerations, including site geometry, the coordination number (CN) of nearest neighbors, and the valence of the absorbing atom. For example, in Fig. 3, an increase in the valence of Fe in the series of FeO (2+)→Fe_3O_4 (mixed 2+ and 3+)→Fe_2O_3 (3+)→Fe-HRP (horseradish peroxidase, 4+) results in a systematic shift of the 1*s*-3*d* edge features toward higher energy. The 1*s*-3*d* edge position for $YBa_2(Cu_{1-x}Fe_x)_3O_{7-\delta}$ is found[14] to be ~2 eV higher than that of Fe^{2+} compounds and ~2 eV lower than that of Fe^{4+} compounds, but very close to that of Fe^{3+} compounds, thus indicating that the valence state of the substitution Fe is mainly +3. Because there is no shift of the edge spectra as Fe content increases, we conclude that the valence of Fe is independent of Fe content.

Our interpretation of the Fe 3*d* edge feature is based on a molecular-orbital theory as described in Ref. 14 and references therein. An important observation for $YBa_2(Cu_{1-x}Fe_x)_3O_{7-\delta}$ is the dependence of 1*s*-3*d* intensities on the doping level (see Fig. 4). For a lower Fe concentration ($x=0.02$ or 2 at. %) the intensity of the 3*d* feature of the Fe-doped sample is about four times larger than that in standard compounds of FeO and Fe_2O_3 with six coordination and twice the size of that in a model

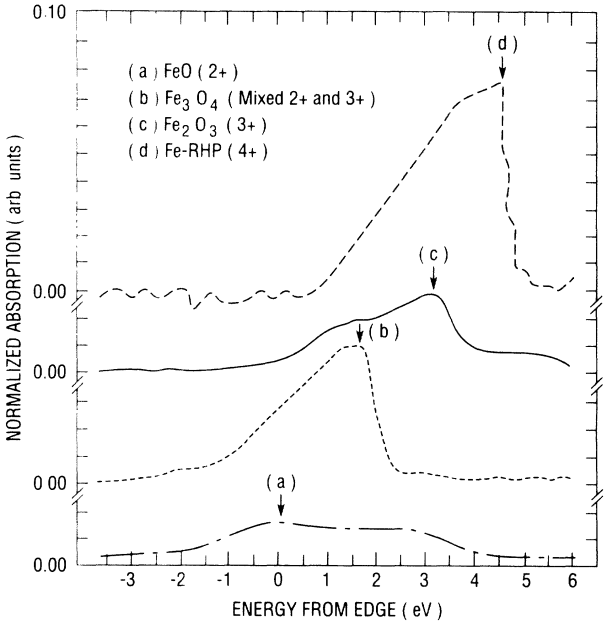

FIG. 3. Fe *K*-edge absorption of 3*d* edge feature for various valence states of iron model compounds: (a) FeO (2+, dot-dashed curve), (b) Fe_3O_4 (mixed 2+ and 3+, short-dashed curve), (c) Fe_2O_3 (3+, solid curve), (d) Fe-HRP (4+, long-dashed curve). The intensities of 3*d* features were determined by subtracting an arctangent function from the previous data (Ref. 14).

compound of Fe-HRP with five coordination. Our previous results[14] and another EXAFS study by Oyanagi *et al.*[15] indicate that Fe takes the Cu(1) chain site mainly with four coordination at lower concentration. The four-fold coordination geometry of the Fe local environment is noncentrosymmetric because of two shorter Fe-O bonds (1.84 Å) along the *c* axis and the other two oxygen neighbors (1.95 Å) in the chain layer. As a consequence, the total amount of Fe 4*p* states can hybridize with the 3*d* states, resulting in a large contribution at the 3*d* position.

EXAFS results[14,15] also show an increase in the number of oxygen neighbors in the linear-chain layer, indicating the presence of extra oxygen atoms on the normally vacant sites of the chain. The change of oxygen coordination number as a function of Fe concentration can also be seen in Fig. 4. When the Fe content increases, the intensities of the 3*d* peaks decrease. As illustrated in Fig. 3, the intensities of 3*d* features of standard compounds decrease with increasing average oxygen coordination number. The detailed discussion of the variation of the 3*d* intensity due to the effects of coordination number can be found in Ref. 14. Based on such arguments, it is reasonable to suggest that the changes of intensity of the 3*d* peak as shown in Fig. 4 as a function of the Fe content in $YBa_2(Cu_{1-x}Fe_x)_3O_{7-\delta}$ are most likely associated with an increase in the number of nearest oxygen neighbors of Fe as measured by EXAFS measurements.[14,15] We further suggest[14] the formation of Fe-O-Fe linkages, which

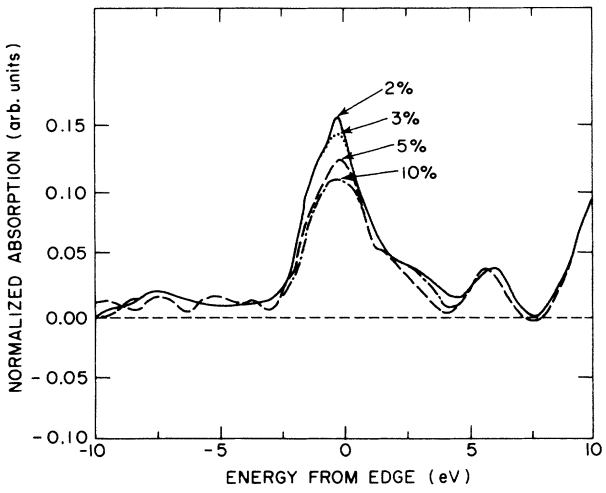

FIG. 4. Variation of 3*d* intensity with Fe concentration. The intensities of 3*d* features were determined by subtracting an arctangent function from the previous data (Ref. 14).

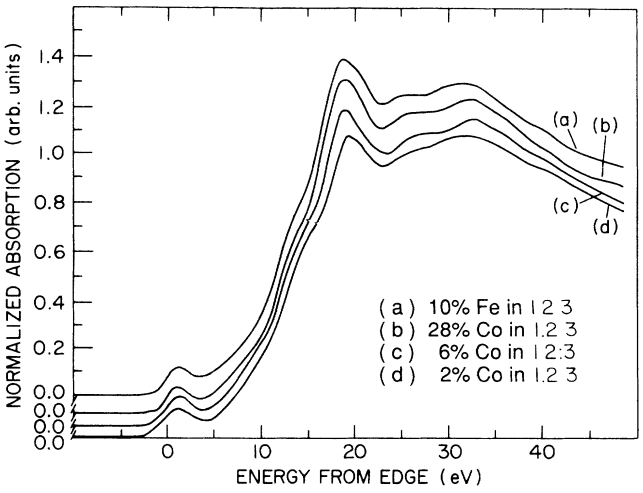

FIG. 5. Comparison of near-edge spectra between Fe- and Co-doped samples: (a) 10 at. % Fe doped in 1:2:3; (b) 28 at. % Co doped in 1:2:3; (c) 6 at. % Co doped in 1:2:3; and (d) 2 at. % Co doped in 1:2:3. The spectrum (a) was measured at Fe *K* edge and others were measured at Co *K* edges.

may be due to strong binding of the extra oxygen to Fe-Fe pairs. A further discussion of the effects of Fe substitution on the changes in crystal and electronic structure is presented in the following subsection.

B. Co *K* edge

Neutron-diffraction studies[17,18] of Co-doped materials agree in general that Co ions substitute on the chain site. Thus, Co behaves like Fe. Our observations are also consistent with this view. The XANES spectra for Fe doping ($x=0.10$) and Co doping ($x=0.02$, 0.04, and 0.28) are compared in Fig. 5. A comparison of the edge energies of Co in $YBa_2(Cu_{1-x}Co_x)_3O_{7-\delta}$ with those of standard compounds, including CoO (2+) and Co_2O_3 (3+) suggests that Co-doped samples have a Co valence of 3+ (data not shown). As one can see in Fig. 5, the valence of Co^{3+}, like that of Fe^{3+}, is independent of composition.

The similarity of the Fe ($x=0.10$) sample to the Co ($x=0.28$) sample is further illustrated by the first derivatives of the edge spectra shown in Fig. 6. The features (*A*, *B*, *C*, *D*, and *E*) of both spectra are very similar with respect to their positions, magnitudes, and shapes. This suggests that both Fe and Co sites have similar electronic structures and local environments for high-doping samples. In Ref. 14, we suggested that Fe has a preference for fourfold and fivefold coordinations. This also holds true for the Co structural configuration. Since the doped Fe and Co are trivalent, it is therefore reasonable to suggest that additional oxygen is drawn into the structure to compensate for the excess charge of Fe^{3+} and Co^{3+} substituted for Cu^{2+}. Our results indicate that the oxygen coordination number (CN) of Fe and Co along the *a* axis increases with increasing Fe and Co contents. Our findings are in good agreement with several neutron measurements.[17–19] From neutron measurements,[17–19] it has been established that, for Fe- and Co-doped samples, oxygen content increases from the pure 1:2:3 value with increasing concentration of dopants. In fact, neutron-diffraction studies have shown[19] that in Fe-doped samples the change in oxygen is approximately $\delta=-3x/2$. For Co substitution the increase in oxygen content may be

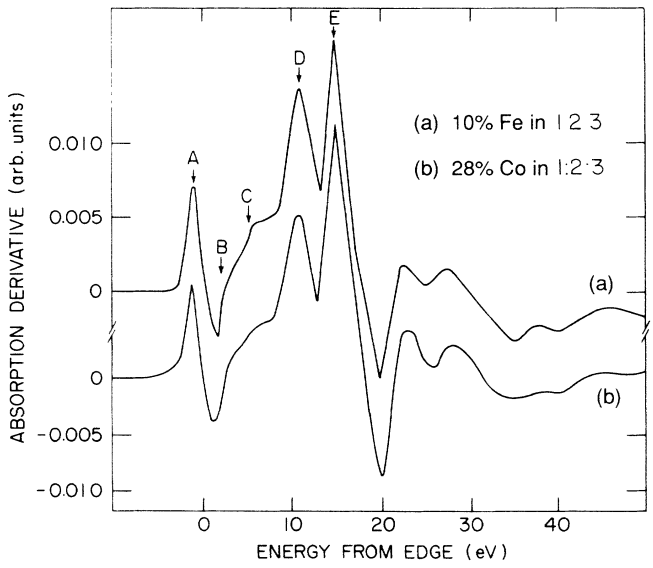

FIG. 6. Further comparison of near-edge spectra, there displaying the first derivative of two spectra from Fig. 5, for (a) 10 at. % Fe doped in 1:2:3 and (b) 28 at. % Co doped in 1:2:3.

slightly less. The effects of Fe and Co substitution on the electronic and atomic structure in 1:2:3 are similar, but do differ to a small degree. Unlike the Fe-doped spectra (see Fig. 4), the intensities of the Co $1s$-$3d$ transition change only slightly with composition (see Fig. 7). Therefore, this additional oxygen attracted to Fe or Co sites must be distributed in a different manner. Another possible explanation is that oxygen content is not identical for the same Fe and Co concentration. However, we should also take into account the fact that these minor differences between Fe and Co samples may also be due to minor variations in sample preparation. Moreover, our Cu XANES spectra[20] as well as those of Ref. 15 show no significant change of the electronic structures of Cu, even for a high concentration of Fe or Co doping. This indicates that the interactions which inhibit charge transfer and alter hole carriers in the chains, and subsequently suppress superconductivity, are of short range near Fe or Co sites.

Fe and Co doping induce an orthorhombic-to-tetragonal phase transition in 1:2:3. A tetragonal phase is also attained by disordering of the oxygen atom from the b sites to the unoccupied a sites or by completely removing this oxygen. It is conceivable that the phase transition of 1:2:3 induced by Fe and Co may be an order-disorder transition. Each Fe^{3+} and Co^{3+} placed at Cu(1) sites will give rise to an additional oxygen. Thus, it is difficult to relate the distribution of oxygen in the a-b plane in Fe- and Co-doped 1:2:3 to that of oxygen-deficient 1:2:3. Several TEM studies[19,21–24] have also been interpreted to show that although the structures of Fe- and Co-substituted 1:2:3 have tetragonal symmetry, microdomains of the orthorhombic structure may remain. Since the presence of Fe and Co in the chains induces additional oxygen, also in the chains, the Fe or Co can have at least three coordination geometries, i.e., fourfold, fivefold, and sixfold. We note that bond lengths (R's) of Fe-O and Co-O pairs of the a-b plane in our observations change little across the orthorhombic-tetragonal phase boundary. However, we do observe additional fivefold and sixfold coordination of dopant sites as dopant content is increased. Thus the macroscopic picture, we suggest, consists of small orthorhombic domains disrupted by those higher-coordination sites (fivefold and sixfold) such that average symmetry is observed to be tetragonal (as in x-ray diffraction).

More sophisticated interpretations of an EXAFS study to explain the orthorhombic-to-tetragonal phase boundary of 1:2:3 by Co and Fe have been made by Bridges *et al.*[25] They support the formation of zig-zag chains due to Co doping from the second shell of Co environments in 1:2:3. This model indicates that the first shell of Co-O pairs is at a long (2.36 Å) and a short (1.84–1.88 Å) distance. However, we find that our data cannot be fitted with their results[25] for the first shell. In fact, our Co samples have different Co-O distances (1.85 Å and 1.95 Å). The discrepancy between their results and our current data is likely to be at least partly a matter of different sample preparation. In addition, there exist significant obstacles[14,26,27] to determining higher-shell information in high-T_c materials using EXAFS as attempted in Ref. 25. Because several contributions from different types of scatterers are situated at nearly the same relative distance, EXAFS data analysis of the higher shells for Co, Fe, and Cu edges are complicated and difficult. Therefore, we feel that the description of zig zags in the chain based on EXAFS high-shell data analysis[25] for Co- and Fe-doped samples is reasonable, but not conclusive.

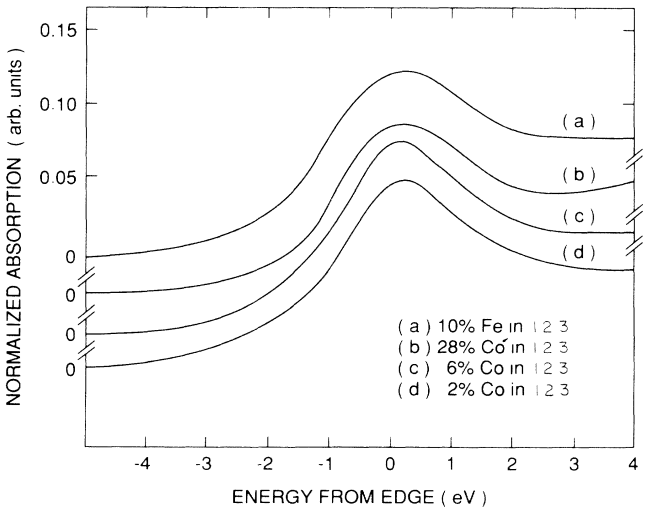

FIG. 7. An expanded view of $3d$ edge features corresponding to Fig. 5.

C. Ni K edge

Contradicting models for the occupancy of the Ni site in Ni-doped 1:2:3 have been proposed. Neutron-diffraction studies[28] found that Ni occupies the Cu(2) site in the CuO_2 planes, but Raman scattering indicated[29] that Ni substitutes into the Cu(1) site in the linear chains. An EXAFS measurement, reported by Qian *et al.*,[30] claimed that it is not possible to locate the Ni atom, which does not substitute for copper, but is in an unknown defect site. A differential anomalous scattering study suggested[31] that Ni atoms occupy the Cu(1) site and the Cu(2) site in a nearly random distribution. Our EXAFS data analysis indicates that there are two Ni sites (in agreement with Ref. 31). Ni at the chain site forms fourfold coordination with bond lengths similar to undoped 1:2:3 Cu chain sites, while Ni at the plane site forms fivefold coordination with appropriate bond lengths. EXAFS results are presented[32] elsewhere.

The Ni K-edge spectra for $YBa_2(Cu_{1-x}Ni_x)_3O_{7-\delta}$ ($x=0.02$, 0.04, and 0.06) are shown in Fig. 8 with the reference compound NiO. The similarity of the energies for two edge features, denoted as A and C, between NiO and Ni-doped samples suggests that Ni is divalent in 1:2:3. The small edge feature A in NiO and Ni-doped samples is assigned to the $1s$-$3d$ transition. As discussed in subsection A, the $3d$ edge features can be used as an in-

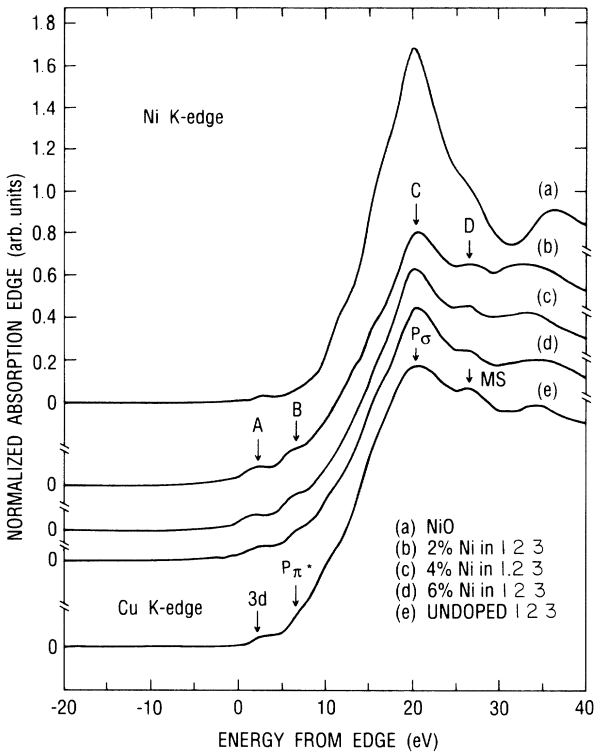

FIG. 8. Ni K-edge absorption near-edge spectra for (a) NiO, (b) 2 at. % Ni doped in 1:2:3, (c) 4 at. % Ni doped in 1:2:3, and (d) 6 at. % Ni doped in 1:2:3. For comparison, Cu K-edge near-edge spectra of an undoped sample are shown in (e). The assignment of each edge feature was adopted from Heald *et al.*, Refs. 33 and 34.

dicator of coordination geometries for absorbing atoms. The data in Fig. 8 show a higher intensity of the $3d$ features for Ni-doped samples in comparison with that of NiO. This is due to the noncentrosymmetric geometries for Ni-doped samples with possible square-planar and square-pyramidal coordination. The peak B of Ni-doped samples is shifted to lower energies and enhanced with respect to that of NiO. The spectra of Ni-doped samples above the main peak C show a distinguishable peak D, which is absent from those of NiO. As one can clearly see, in Fig. 8 there is no resemblance between the shapes of NiO and Ni-doped spectra. Therefore, we rule out the possibility that a significant fraction of the NiO phase contaminates in our Ni-doped samples. Qian *et al.*[30] reported contamination by NiO in their EXAFS spectra of Ni-doped 1:2:3. The discrepancy between current data and their results[30] may be a matter of sample differences.

In order to better understand the edge features for the Ni-doped spectra, it is also instructive to make a comparison between the shapes of these spectra and that of the Cu K-edge spectrum for undoped 1:2:3 as shown in the bottom of Fig. 8. Note that the shape of the Ni K-edge spectra of Ni-doped samples is similar to that of the Cu K-edge spectrum of undoped 1:2:3. This is consistent with our EXAFS observations, which show[32] the similarity of the radial distribution between Ni-doped samples and undoped 1:2:3 at the Cu K edge. Heald *et al.*[33,34] have reported XANES measurements of Cu K-edge spectra for different orientations of aligned 1:2:3. A clear demonstration of assignment of the edge features, in particular to the peaks B and D, to different Cu site geometries has been made.[33,34] We apply those arguments from Heald *et al.*[33,34] to the Ni-doped spectra. The edge feature B for Ni-doped samples is assigned to the transition to $4p_{\pi^*}$ states with shakedown contributions, which are associated with the charge transfer from the oxygen to nickel. The peak B ($4p_{\pi^*}$ states) is particularly enhanced in square-planar (fourfold) geometry.[35] We speculate that this peak B in Ni-doped samples occurring at lower energies is associated with some of the Ni atoms located in Cu(1), the linear-chain site. The main peak C at the top of the edge is attributed to transition to $4p_\sigma$ states. The edge feature D is associated with EXAFS contributions from high-shell neighbors. Like that of the Cu K edge for undoped 1:2:3, we argue that the presence of the peak D, as the signature of the EXAFS multiple scattering (MS) within the CuO_2 plane, indicates that some of the Ni atoms reside in Cu(2), the plane site. Therefore, by coupling with previous EXAFS findings[32] and current XANES results, we conclude that Ni atoms substitute for both Cu(1) and Cu(2) atoms. It appears that the size of the $3d$ feature in Ni-doped samples becomes smaller with increasing Ni content. We suggest an increase of the fivefold coordination of Ni with increasing Ni content because of more substitutions onto Cu(2).

D. Zn K edge

Like Ni substitutions, the situation of Zn doping is also controversial regarding the location of the dopant site. There have been various interpretations among neutron-diffraction studies. Xiao *et al.*[4] and Maeda *et al.*[36] concluded that all Zn ions go to the plane sites, while Kajitani *et al.*[28] and Roth *et al.*[37] suggested that Zn atoms occupy both Cu(1) and Cu(2). Our studies support the picture that Zn substitutes only for Cu(2) atoms, the plane sites.

The XANES spectra of Zn, ZnO, and $YBa_2(Cu_{1-x}Zn_x)_3O_{7-\delta}$ ($x=0.01$, 0.02, and 0.04) are presented in Fig. 9. The lower energy part (within 10 eV above the threshold) of the edge spectra of Zn-doped in 1:2:3 closely follows that of ZnO, suggesting that Zn is divalent. In the case of ZnO and Zn doped samples, there is no $3d$ edge feature because of a completely filled d^{10} configuration of Zn^{2+}. The edge features occurring halfway up to the edge (A) and the main peaks (B) for ZnO and Zn-doped samples correspond to the transitions to unfilled $4p$ states with different configurations. Above the main peak B, the spectra of Zn-doped samples show a distinguishable peak (C) at ~ 13 eV. This feature C is absent from spectra of ZnO. We suggest that the presence of this feature C, which is an indicator of the EXAFS MS events within the planes, is evidence that Zn substitutes for Cu(2) at the plane site. In comparison with other spectra as shown in Figs. 5 and 8, the near-edge features

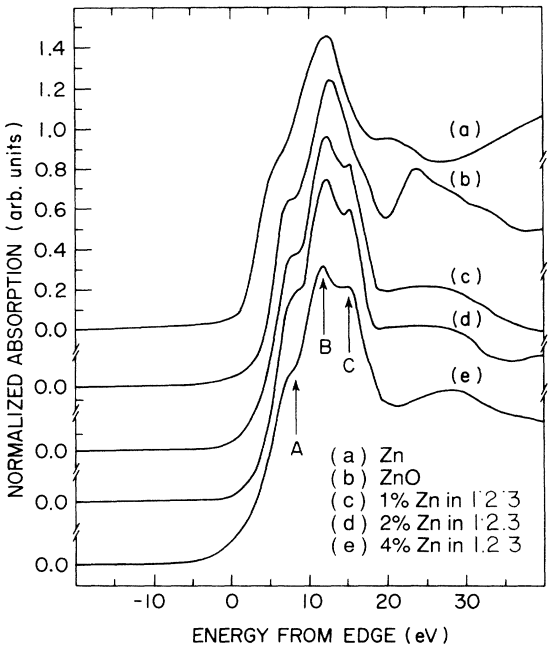

FIG. 9. Zn *K*-edge absorption near-edge spectra for (a) Zn, (b) ZnO, (c) 1 at. % Zn doped in 1:2:3, (d) 2 at. % Zn doped in 1:2:3, and (e) 4 at. % Zn doped in 1:2:3.

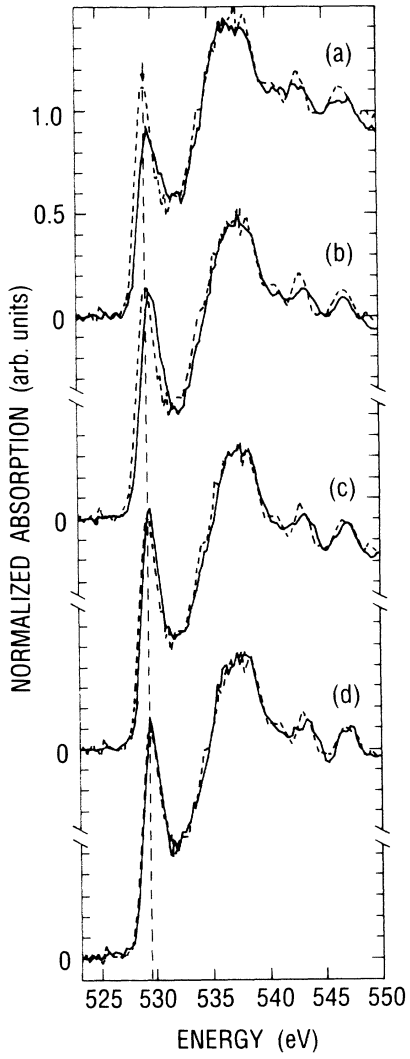

FIG. 10. Comparison of the oxygen *K*-edge near-edge spectra of 4 at. % metal-doped samples (solid curve) with undoped 1:2:3 (dashed curve). From top to bottom they are (a) 4 at. % Fe, (b) 4 at. % Co, (c) 4 at. % Ni, and (d) 4 at. % Zn.

of the Zn-doped spectra (Fig. 9) are totally different from those of other samples including undoped 1:2:3. The large difference may be due to the absence of chain features in Zn-doped spectra (Fig. 9). EXAFS data analysis shows[32] that the contributions of the first shell are due to substitutions of Zn at the plane sites with four equal length and one longer Zn-O bonds. Our EXAFS findings[32] agree with neutron diffraction and EXAFS measurements by Maeda *et al.*[36] Mechanisms which may cause the large suppression of T_c particular to Zn-doped samples are discussed in the following subsection.

E. O *K* edge

Figure 10 presents a comparison of the O *K*-edge near-edge spectra between $YBa_2(Cu_{0.96}M_{0.04})_3O_{7-\delta}$ (M = Fe, Co, Ni, and Zn; solid line) and undoped 1:2:3 (dashed line). The peaks above the threshold correspond to the transition from the core level to unoccupied O($2p$) states near the Fermi level. The effects of metal doping on the O($2p$) states can be seen in Fig. 10. First, the first peaks shift to high energy in the 4 at. % Fe-doped, 4 at. % Ni-doped, and 4 at. % Co-doped samples, while the energy is unaffected by 4 at. % Zn doping. Second, the intensity of the first peak is reduced in the Fe-doped sample, while the peaks of Co-, No-, and Zn-doped samples change little. These effects can be more clearly seen in the difference spectra (shown in Fig. 11) between 4 at. % metal-doped and undoped samples.

The first peak (see Fig. 10) occurring near 528.5 eV just above the threshold has been identified[7,38–40] as the hole states near the Fermi level. We believe that for Fe-, Co-, and Ni-doped samples the changes of some hole states may explain the positive shift of the peak positions near the threshold with respect to that of undoped 1:2:3 as shown in Fig. 10. It is most striking that within experimental uncertainties the oxygen $2p$ states change little, if any, in the Zn-doped sample. Our observation of the oxygen spectrum for Zn substitution is in good agreement with that of denBoer *et al.*[40]

In the following, we consider several possible mechanisms responsible for suppressing T_c. We should first take into consideration that substitution of Cu(2) by Zn and partly by Ni leads to a greater decrease of T_c than replacement of Cu(1) by Fe and Co. This is due to the fact that the obstruction of charge distribution in the CuO_2 planes is much more effective for T_c suppression. This may explain why the transition temperature for Zn substitution decreases more rapidly than that of other substitutions (simply because all Zn ions are on plane sites).

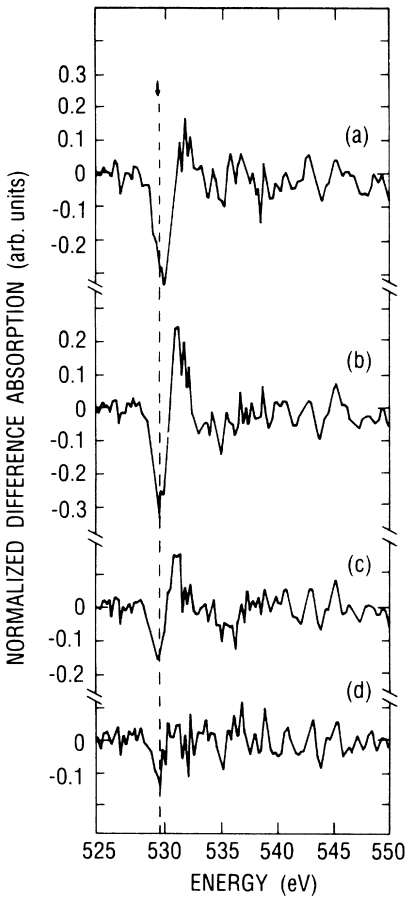

FIG. 11. Difference (between undoped 1:2:3 and 4 at. % metal-doped samples) spectra corresponding to Fig. 10.

Tokura *et al.*[8] have suggested that holes in the chain region are localized, while holes in the plane are mobile. As noted above, there is site preference for substitutions onto chains for Fe and Co, as well as partly for Ni. Although superconductivity is largely determined by planar conduction, the substitutions into the chains by Fe, Co, and partly by Ni will lead to a redistribution of holes in the chain region and possibly an inhibition of charge transfer from the chains to the planes. This is consistent with the idea[8] that chains provide a reservoir of charge.

It is clear that each dopant has a different effect on the oxygen $2p$ states, as shown in Figs. 10 and 11. We suggest several factors that may come into play in metal-doping cases. Since this peak has been identified as due to hole states near the Fermi level by several research groups,[7,38–40] it is reasonable to suggest that the changes of the oxygen $2p$ states for Fe-, Co-, and Ni-doped samples may be related to a reduction of some oxygen hole states. This is consistent with Hall measurements.[9] In addition, we believe that the change of oxygen coordination can certainly affect the intensity of the oxygen $2p$ peak, especially concerning the Fe- and Co-doping cases. Our data indicate that qualitatively, Fe is more effective in the reduction of oxygen holes than Co, Ni, and Zn. This can be partly explained by the fact that Fe^{3+} and Co^{3+} enter the Cu(1) and alter the local oxygen environment to compensate the charge for Cu^{2+}. This has been discussed in subsections A and B. We speculate that this extra oxygen in Fe-doped samples may be distributed in a different way from those of Co-doped samples and, therefore, may behave chemically differently to affect the charge distribution. As a result, different effects on the oxygen hole states in the chains for the Fe-doped sample have been indicated in Figs. 10 and 11.

The change of oxygen hole states, however, alone cannot explain the suppression of superconductivity in all metal-doping cases. Specifically, Zn substitution is unique because an increase in charge carriers[9,10] is not accompanied by a change in the oxygen hole states, as shown in Figs. 10 and 11. Two questions arise: How is charge distribution in the CuO_2 plane disturbed, and why does the number of holes increase in Zn-doped samples? We are unable, however, to give direct answers from current data.

To address the mechanism causing the large suppression of T_c in the Zn-doping case, we offer several possible explanations, including pair breaking, structural effects, and modifications of band structure. Although the hole concentration is one important factor in achieving high T_c, pairing hole carriers[7,43–46] through Cu-O-Cu interactions are a key factor in determining the superconducting properties of 1:2:3. The presence of Zn in the structure leads to the breakdown of hole pairs.[47] The pair breaking can occur due to weakened Coulomb interactions or magnetic interactions on the Cu(2) plane site by substitutions of Zn onto the Cu(2) site. On the basis of the electronic configuration of Zn ($d^{10}sp^3$), the d levels do not take part in the orbitals utilized. There is a possibility[48] for the bond arrangement of Zn sites to form a flattened tetrahedral configuration in the plane with a fifth bond along the c axis, which structurally is quite unlike the square-pyramidal coordination of Cu(2) atoms. Structural disorder on the Zn site may disrupt the superconducting transport path. However, due to difficulties in obtaining higher-shell information, our current EXAFS data[32] cannot confirm this point. The lack of hybridization between Zn ($3d$) and O ($2p$) orbitals certainly affects the conduction band, and thus the effective hole concentration may increase by doping of Zn. It has been demonstrated[8–10] that to achieve higher T_c one should not correlate with the total hole concentration, but only with an optimum hole concentration. Although the hole concentration increases in the Zn-doping case, other *killing* factors are sufficient to suppress superconductivity. Further study is needed for a comprehensive understanding of the variation of T_c with dopants.

IV. SUMMARY

We have examined the effects of the metal doping (Fe, Co, Ni, and Zn) in 1:2:3 using x-ray absorption near-edge spectroscopy. While no simple unified picture of these substitutions can explain the chemical and physical properties observed, our studies and results demonstrate that several factors relate intimately with changes of superconductivity. These factors are the location of dopants,

TABLE II. Brief summary of the influence of metal substituents on the location of dopants, the valence of dopants, structural changes, and the distribution of holes.

Metal:	Fe	Co	Ni	Zn
Location:	Chain	Chain	Chain and plane	Plane
Valence:	$3+$ ($3d^5$)	$3+$ ($3d^6$)	$2+$ ($3d^8$)	$2+$ ($3d^{10}$)
M-O bond:	Fe-O (Refs. 14 and 32)	Co-O (Ref. 32)	Ni-O (Ref. 32)	Zn-O (Ref. 32)
R (Å):	(1.84 and 1.95)	(1.85 and 1.95)	(1.82, 1.97, and 2.29)	(2.0 and 2.3)
CN with x:	Increase	Increase	a	a
Oxygen content:	Increase (Ref. 19)	Increase (Ref. 17)	a	a
Oxygen $2p$ states:	Change	Change	Change	No change
Hole concentration:	Decrease (Ref. 9)	Decrease (Ref. 9)	Decrease (Ref. 9)	Increase (Refs. 9 and 10)

[a]Indeterminate.

the valence of dopants, structural changes, modifications of electronic densities of states, and the distribution of holes. The results are summarized in Table II. Our previous EXAFS measurements,[14,32] considered with current near-edge spectra, support the view that Fe and Co preferentially substitute for the Cu(1) atom at the linear-chain site; Ni resides both at the Cu(1) chain site and the Cu(2) plane site; and Zn only occupies in the plane position, Cu(2). It is clear that each Cu site plays a different role in terms of charge distribution and superconductivity. The similarity of Fe-O bond distances (1.84 Å and 1.95 Å) and Co-O bond distances (1.85 Å and 1.95 Å) is indicated in Table II. Furthermore, as indicated in Table II, our results show that there are two Ni sites. Ni at the chain site forms fourfold coordination with bond lengths (1.82 Å and 1.97 Å) similar to undoped 1:2:3 Cu chain sites, while Ni at the plane site forms fivefold coordination with appropriate bond lengths (1.97 Å and 2.29 Å). We find that for the Zn-doped samples the contributions of the first shell are due to substitutions of Zn at the plane sites with four equal length (2.0 Å) and one longer Zn-O bonds (2.3 Å). In all cases, the metal-oxygen bond lengths (Fe-O, Co-O, Ni-O, and Zn-O) and valence states of each dopant (mainly Fe^{3+}, Co^{3+}, Ni^{2+}, and Zn^{2+}) show little dependence on dopant concentration (x). However, the oxygen coordination number (CN) of Fe and Co increases with increasing Fe and Co content. We suggest that an excess of oxygen is drawn into the structure for Fe- and Co-doped samples in order to compensate for the excess charge of Fe^{3+} and Co^{3+} substituted for Cu^{2+}. This is in good agreement with neutron measurements,[17,19] which show an increase of oxygen content in Fe- and Co-doped samples. Each dopant affects to a different degree the oxygen $2p$ states. We propose that the changes of oxygen $2p$ states for Fe-, Co-, and Ni-doped samples (see Figs. 10 and 11) may be related to a reduction of some oxygen hole states, which is thought to be an important mechanism suppressing T_c. This is consistent with Hall measurements.[9] We believe that the reduction of some oxygen hole states is attributed to a redistribution of charge carriers in the chain layer and an inhibition of charge transfer from the chains to the planes. However, Zn substitution is unique because an increase in charge carriers,[9,10] is not accompanied by a change in the oxygen $2p$ states as shown in Figs. 10 and 11, indicating that Zn substitution has a different mechanism for suppression of T_c. We speculate that the large T_c suppression in the Zn-doped case may be associated with the breakdown of hole pairs, local structural changes, and the modifications of band structure.

ACKNOWLEDGMENTS

The authors are grateful to J. M. Tranquada and V. J. Emery for valuable discussions. Our special thanks also go to S. P. Craner for his assistance in using the 13-element Ge detector. Support for this research was provided by the Office of the U.S. Department of Energy under Contract No. DE-AC02-76CH0016.

*Present address: AT&T Bell Laboratories, Holmdel, NJ 07733.

[1]Y. Maeno *et al.*, Nature (London) **328**, 512 (1987); Y. Maeno *et al.*, Jpn. J. Appl. Phys. **26**, L1982 (1987).

[2]G. Xiao *et al.*, Phys. Rev. B **35**, 8782 (1987); Nature (London) **332**, 238 (1988).

[3]J. M. Tarascon *et al.*, Phys. Rev. B **36**, 8393 (1987); **37**, 7458 (1988).

[4]A. A. Arbrikosov and L. P. Gok'ov, Zh. Eksp. Teor. Fiz. **39**, 1781 (1961) [Sov. Phys.—JETP **12**, 1243 (1961)].

[5]L. F. Mattheiss and D. R. Hamann, Solid State Commun. **63**, 395 (1987).

[6]V. J. Emery, Phys. Rev. Lett. **58**, 2794 (1987).

[7]N. Nücker *et al.*, Phys. Rev. B **37**, 5185 (1987); **39**, 6619 (1989).

[8]Y. Tokura *et al.*, Phys. Rev. B **38**, 7156 (1988), and references

therein.
[9]N. Okazaki *et al.*, in *Proceedings of the 1988 Materials Research Society International Meeting on Advanced Materials, Tokyo, 1988* (Materials Research Society, Pittsburgh, 1988), p. 737.
[10]M. W. Shafer *et al.*, Phys. Rev. B **39**, 2914 (1989).
[11]C. Y. Yang, J. E. Penner-Hahn, and P. M. Stefan, Nucl. Instrum. Methods (to be published).
[12]S. P. Cramer *et al.*, Nucl. Instrum. Methods **A266**, 5816 (1988).
[13]D. A. Fischer *et al.*, Rev. Sci. Instrum. **60**, 1596 (1989); D. A. Fischer *et al.*, Mater. Res. Soc. Symp. Proc. **143**, 139 (1989); D. A. Fischer *et al.*, Surf. Sci. **177**, 114 (1986).
[14]C. Y. Yang *et al.*, Phys. Rev. B **39**, 6681 (1989); C. Y. Yang *et al.*, Physica B **158**, 486 (1989).
[15]H. Oyanagi *et al.*, Jpn. J. Appl. Phys. (to be published).
[16]V. C. Srivastara and H. L. Nigan, Coord. Chem. Rev. **9**, 275 (1972–1973).
[17]P. Zolliker *et al.*, Phys. Rev. B **38**, 6575 (1988).
[18]Y. K. Tao *et al.*, J. Mater. Res. **3**, 248 (1988).
[19]Yuwen Xu *et al.*, Phys. Rev. B **39**, 6667 (1989).
[20]C. Y. Yang *et al.* (unpublished).
[21]T. Ichitiashi *et al.*, Jpn. J. Appl. Phys. **27**, 1594 (1988).
[22]G. V. S. Sastry, R. Wordenweber, and H. Freyhardt, J. Appl. Phys. **65**, 3975 (1989).
[23]Z. Hiroi *et al.*, Jpn. J. Appl. Phys. **27**, 1580 (1988).
[24]G. Roth *et al.*, Z. Phys. B **71**, 43 (1988).
[25]F. Bridges *et al.*, Phys. Rev. B **39**, 11 603 (1989).
[26]C. Y. Yang *et al.*, Phys. Rev. B **36**, 8798 (1987).
[27]C. Y. Yang *et al.*, Phys. Rev. B **38**, 6568 (1988).
[28]T. Kajtiani *et al.*, Jpn. J. Appl. Phys. **27**, L354 (1988).
[29]Z. Iqbal *et al.*, Phys. Rev. B **36**, 2283 (1987).
[30]M. Qian *et al.*, Phys. Rev. B **39**, 9192 (1989).
[31]R. S. Howland *et al.*, Phys. Rev. B **39**, 9017 (1989).
[32]C. Y. Yang *et al.*, in *Proceedings of the 1989 Materials Research Society Meeting, Boston, 1989* (Materials Research Society, Pittsburgh, in press).
[33]S. M. Heald *et al.*, Phys. Rev. B **38**, 761 (1988).
[34]S. M. Heald *et al.*, Physica B **158**, 433 (1989).
[35]N. Kosugi *et al.*, Chem. Phys. **91**, 249 (1984).
[36]H. Maeda *et al.*, Physica C **157**, 483 (1989).
[37]G. Roth *et al.*, Physica C **162-164**, 518 (1989).
[38]J. A. Yarmoff *et al.*, Phys. Rev. B **36**, 3967 (1987).
[39]P. Kuiper *et al.*, Phys. Rev. B **38**, 6483 (1988).
[40]M. L. denBoer *et al.*, Phys. Rev. B **38**, 6588 (1988).
[41]L. A. Grunes *et al.*, Phys. Rev. B **25**, 7157 (1982).
[42]F. M. F. de Groot *et al.*, Phys. Rev. B **40**, 5715 (1989).
[43]*Theories of High Temperature Superconductivity,* edited by J. W. Halley (Addison-Wesley, New York, 1988), and references therein.
[44]J. H. Hirsch *et al.*, Phys. Rev. Lett. **60**, 1668 (1988).
[45]Y. Gao, J-M. Langlois, and W. A. Goddand III, Science **239**, 896 (1988).
[46]A. Aharony *et al.*, Phys. Rev. Lett. **60**, 1330 (1988).
[47]V. J. Emery (private communication).
[48]A. F. Wells, *Structural Inorganic Chemistry* (Clarendon, Oxford, 1975).